Agric Res J **60** (2) : 255-261, *April* 2023
DOI No. 10.5958/2395-146X.2023.00039.X

AN IMPROVED SOLAR AIR HEATER FOR POST HARVEST APPLICATIONS

V S Hans*, R S Gill and Rupinder Pal Singh

Department of Mechanical Engineering, Punjab Agricultural University, Ludhiana-141004, Punjab

ABSTRACT

Farmers incur huge losses every year on account of post harvest losses. Use of solar dryers helps in reducing the post-harvest losses by improving quality and shelf life. A solar air heater is an important component of a solar dryer and its performance is improved with the application of heat transfer enhancement techniques. The enhancement in heat transfer of rectangular ducts having a configuration of broken arc ribs roughness is determined for Reynolds number ranging from 2000-16000. Two gaps equal to rib height were provided symmetrically in continuous arc-rib. Five broken arc rib roughened plates having relative gap position in the range of 0.2-0.8 (five values) have been tested. The arc angle and relative roughness height were fixed as 30° and 0.043, respectively. The maximum enhancement of heat transfer as compared to smooth duct is found to be 155.4% more for *d/w* of 0.65 and *Re* of 12000.

Keywords*:* Broken arc rib roughness, Heat transfer enhancement, Post harvest losses, Solar air heater, Solar drying

www.IndianJournals.com
Not for Commercial Use
Downloaded From IP - 216.73.216.57 on dated 15-Nov-2026

India is the second largest producer of rice, wheat, sugarcane, cotton and groundnuts, as well as a fruit and vegetable producer, accounting for 10.9% and 8.6% of world fruit and vegetable production, respectively. As per the report of "Committee for doubling of farmers' income" farmers incur a loss of Rs 92,651 crore per year due to post-harvest losses. The committee recommended development of infrastructure near-farm aggregation points for post-harvest processing of fresh produce. Solar dryers are efficient alternative to open sun drying for removing the moisture which improves quality and shelf life. Solar dryer has many applications in drying agricultural products, such as seeds, fruits and vegetables (Hans et al., 2014; Dutta and Kumar, 2017; Komolafe *et al.*, 2019). A solar air heater (SAH) is an important component of a solar dryer as it is used for heating air by utilizing solar energy. Conventional solar air heaters mainly consist of glazing with a plate forming a passage for air flow with plate acting as an absorber. SAH is insulated thermally from the back and the sides. The only drawback of flat solar heaters is their low thermal efficiency because of low heat transfer between the absorber plate and air. Different modifications such as use of porous absorber, corrugated absorber, finned absorber, artificially roughened absorber, etc. in the air flow passage of conventional solar air heater have been suggested by many investigators to enhance heat transfer between the absorber plate and air, thus, its thermal efficiency (Sukhatme, 1996; Chhaparwala, 2019; Komolafe *et al.*, 2019; Sivakandhana *et al.*, 2020). The use of artificial roughness on the underside of absorber plate of conventional solar air heater has found to be one of the most effective and economic way of improving the thermal performance of a solar air heater (Varun *et al.*, 2007; Hans, 2010; Bhushan and Singh, 2010; Gupta and Varshney, 2017; Kant and Saini, 2018). The presence of ribs on absorber breaks low heat transfer viscous sub-layer and creates turbulence close to wall, thereby enhancing the thermal performance of SAH.

The rib roughness geometries such as transverse, inclined, V-shape, arc-shape, S-shape, and random shapes have been investigated in detail by many investigators. In the beginning, the studies related to the effect of SAH ducts roughened with transverse ribs on heat transfer and friction factor were conducted by Han *et al.* (1978). After this, it was revealed that placing continuous ribs inclined to the mainstream flow perform better than the transverse rib due to generation of two counter rotating secondary flow cells resulting in increase in local heat transfer (Karwa, 2003; Han and Park, 1988). Park et al. (1992) also reported significantly greater heat transfer enhancement in case of inclined rib to that of transverse ribs. With further investigation to find high performance ribs, Han *et al.* (1991) tested the performance of V-up, and V-down ribs and found that continuous V-shaped ribs perform better than the continuous inclined ribs. Hans *et al.* (2010) further concluded that continuous multi V-shape ribs has more heat transfer rate than the inclined and single V rib due to generation of more counter rotating secondary flow cells. In other attempts, Sahu *et al.* (2005), Aharwal (2008), Kumar *et al.* (2011) and Singh *et al.* (2012) claimed that enhancement in heat transfer can be obtained with no significant increase in the pressure drop by introducing a gap in continuous inclined, V

*Corresponding author : vishiihans@pau.edu
Date of receipt: 17.12.2020, Date of acceptance: 06.08.2021

and multiple V ribs. This is due to generation of more number of secondary flow cells in case of rib with gap as compared to a continuous rib and interruption of growth of boundary layer downstream of a rib as secondary flow passes through the gap.

The above literature survey reveals that no study on the effect of gap position on thermal performance of a solar air heater roughened artificially with of broken arc rib has been carried out so far. It has, therefore, been felt that there is a need to study effect of variation in relative gap position of broken arc-shape circular ribs on the Nusselt number and friction characteristics of solar air heater. The rib-roughness geometry, experimental details, data reduction and results are presented in the following sections.

MATERIALS AND METHODS

For application of rib roughness pertaining to solar air heaters, only one side of the absorber is roughened artificially with rib roughness created by fixing aluminium wires of circular cross-section on air flow side of the absorber. The general geometry of broken arc rib roughness is shown in Fig. 1. The rib roughness can be described by the values of rib height (*e*), rib pitch (*P*), and half width of duct (*w*). A gap (*g*) equal to rib height was provided symmetrically in both legs of arc-shape having gap position (*d*) from upstream edge of arc. These roughness parameters in dimensionless form have been written as relative roughness pitch (*P/e*), relative arc angle (α/90), relative gap position (*d/w*), relative gap width (*g/e*), and relative roughness height (e/D_h). The investigation was carried out to determine Nusselt number and friction factor due to change in relative gap position (*d/w*). Five roughened plates were prepared for relative gap position (*d/w*) of 0.2, 0.35, 0.5, 0.65 and 0.8 as shown in schematic diagrams of Fig. 2. The other roughness parameter such as α/90, *P/e*, *g/e* and e/D_h for present study were selected as 0.333, 8, 1.0 and 0.043 respectively. Table 1 show the values of flow and roughness parameters considered in this study.

Table 1. Values of flow and roughness parameters

Parameters	Range
Reynolds Number (Re)	2000 to 16000
Relative gap position (d/w)	0.20, 0.35, 0.5, 0.65, 0.8
Relative roughness pitch (p/e)	8
Wire arc-angle (α), degree	30°
Relative arc angle, (α/90)	0.3333
Relative gap width (g/e)	1.0
Relative roughness height (e/D_h)	0.043

An indoor test facility (Fig. 3), having a rectangular duct of 2440 mm length with a air flow cross-section of 300 mm x 25 mm (WxH) has been designed as per guidelines given in ASHRAE standard (ASHRAE, 1977) to see the effect of relative gap position of broken arc

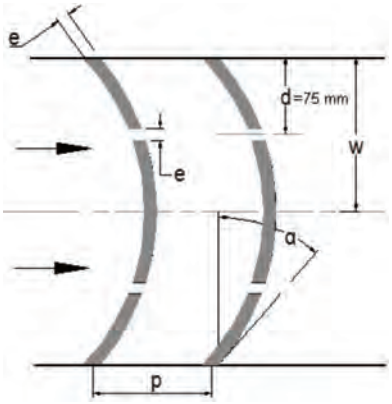


Fig. 1. General arrangement of arc-shaped rib with gap

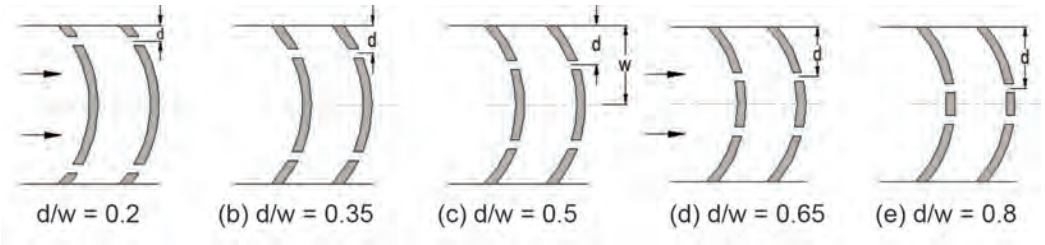


Fig. 2. Schematic diagrams of the arc rib having gap for different relative gap positions

www.IndianJournals.com
Not for Commercial Use
Downloaded From IP - 216.73.216.57 on dated 15-Nov-2026

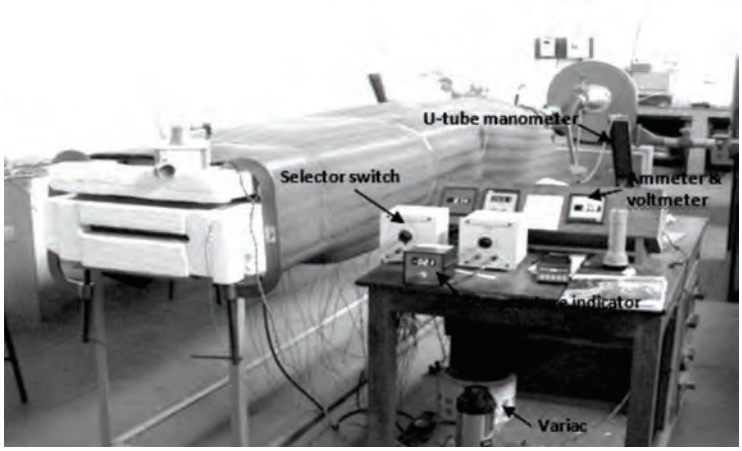


Fig. 3. Photographic View of the Experimental Set-up

www.IndianJournals.com
Not for Commercial Use
Downloaded From IP - 216.73.216.57 on dated 15-Nov-2026

rib on thermal performance of rectagular duct. The duct has three sections namely, entry, test and exit section of length 550 mm, 1000 mm and 890 mm respectively which are more than minimum entry and exit lengths recommended by ASHRAE, (1977). To supply heat to the absorber plate, the Ni-Cr electric heating element is wrapped on the upper surface (1 mm thick). The electric heater is adjusted to 1000 W/m^2 using a variac to get desired temperature rise of absorber. The calibrated digital voltmeter (Make: Scientico; least count of 0.1V) and an ammeter (Make: Scientico; least count of 0.01A) are used to measurement of voltage and current of electrical power supplied to the heater. The entire length of the rectangular duct is insulated by means of 50 mm thick polystyrene (Thermo Cole) having thermal conductivity of 0.037 W/m-K followed by black foam sheet of 10 mm thickness, to ensure minimum heat losses to the environment. The details of the experimental setup, experimental procedure, and equations for computing Nusselt number and friction factor are described comprehensively in previous publication by the authors (Hans *et al.*, 2014). For all the rib-roughened plates investigated, the maximum estimated uncertainties in Reynolds number, Nusselt number and friction factor were ± 2.24%, ± 1.96% and ± 5.17%, respectively at *Re* = 2000 and the corresponding values at the *Re* = 16,000 were ± 1.57%, ± 4.28% and ± 3.48% respectively.

Experimentation on roughened plates has been preceded by validation of the experimental setup. The validation study is conducted by evaluating the Nusselt number (Nu_s) and friction factor (f_s) for smooth duct. The obtained experimental values at different Reynolds number (2000-16000) are compared with proposed correlation by Roshenow *et al.* (1998) and Bhati & Shah (1987). The plots of these comparisons are presented in Figs. 4. The maximum error of ± 3.9 % in Nu_s and ± 2.5% in f_s is obtained.

RESULTS AND DISCUSSION

Figs. 5 and 6 show the variation of Nusselt number and friction factor with Reynolds number for different values of relative gap position (*d/w*) and for fixed values

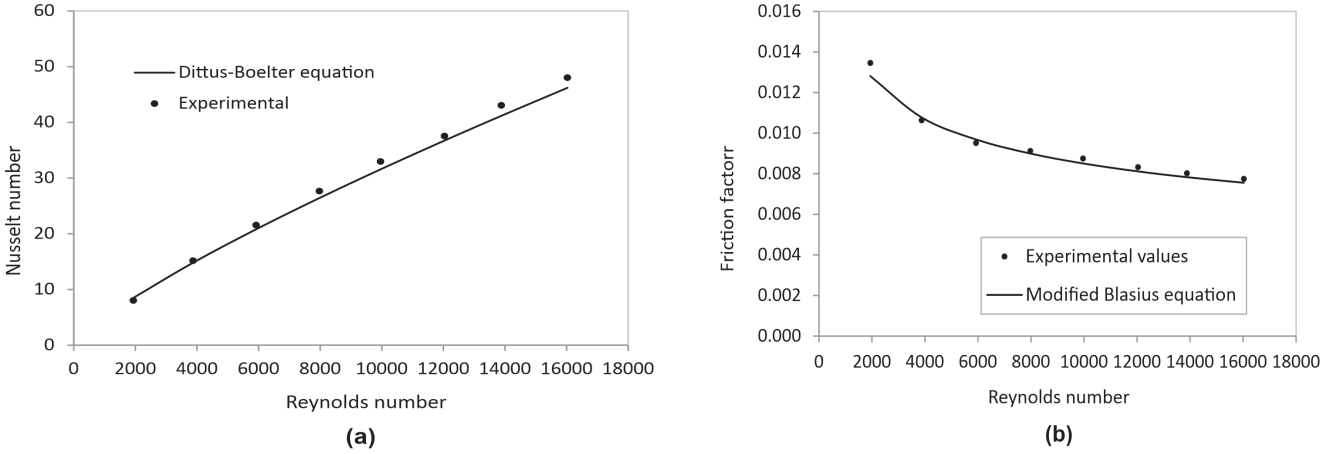


Fig. 4. (a) Nusselt number (b) friction factor comparison between predicted and experimental data for smooth duct.

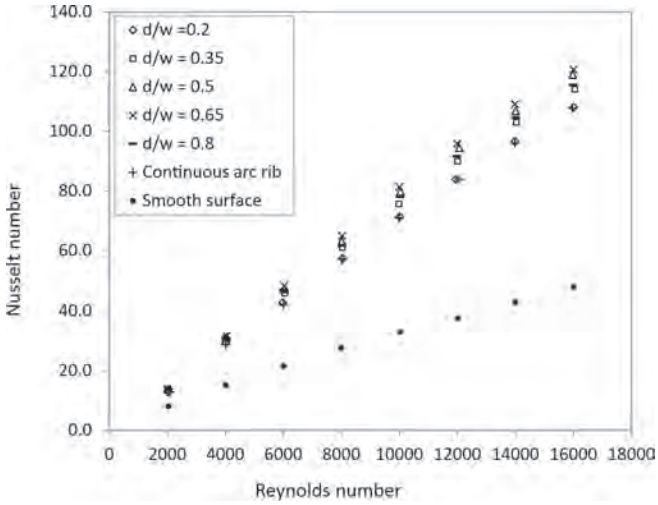


Fig. 5. Nusselt number as a function of Reynolds number for different values of relative gap position (d/w)

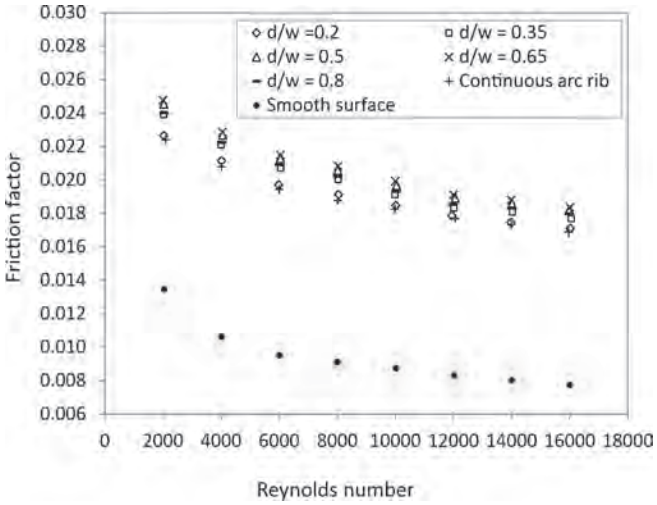


Fig. 6. Friction factor as a function of Reynolds number for different values of relative gap position (d/w)

www.IndianJournals.com
Not for Commercial Use
Downloaded From IP - 216.73.216.57 on dated 15-Nov-2026

of other roughness parameters viz., relative roughness pitch of 8, arc angle of 30°, relative gap width of 1.0 and relative roughness height of 0.043. For comparison, the corresponding results of continuous arc rib roughened duct and smooth duct have also been drawn in respective figures. The Nusselt number and friction factor for broken arc rib are higher than continuous arc rib for all Reynolds number values. This could be due to gap in continuous rib that accelerates the air flow through gap and causes flow-mixing and turbulence in front of the gap as shown in Fig. 7. This increased turbulence in front of the gap enhances local Nusselt number and friction factor thereby, increasing average Nusselt number and friction factor. It can also observed from Figs. 5 and 6 that for all Reynolds numbers, the maximum values of Nusselt number and friction factor are observed at d/w of 0.65. The results are in general agreement with previous investigations by Han et al., 1978 and Han *et al.* (1991).

In order to compare values of the Nusselt number and friction factor of the roughened duct with that of the smooth duct, the values of the Nusselt number enhancement (*Nu/Nus*) and friction factor enhancement (*f/fs*) are presented in Figs. 8 and 9 respectively. From Fig. 8 and Fig. 9, it is observed that Nusselt number enhancement varies from 1.68 to 2.37 and friction factor enhancement varies from 1.62 to 2.55 for the range of flow and roughness parameters investigated. It is observed that the maximum value of enhancement comes at relative gap position of 0.65 for both Nusselt number and friction factor. It is also observed from Fig. 8 and Fig. 9 that as relative gap position increases from 0.20 to 0.65, the Nusselt number and friction factor enhancement increases and then with further increase in relative gap position from 0.65 to 0.80, it decreases. This variation in Nusselt number depends on the strength of secondary flow through gap which further depends on two factors. First factor is interaction of boundary layer on upstream side of the rib with secondary flow moving along the rib, and the second factor is change of angle at which boundary layer strike the arc rib. As the relative gap position

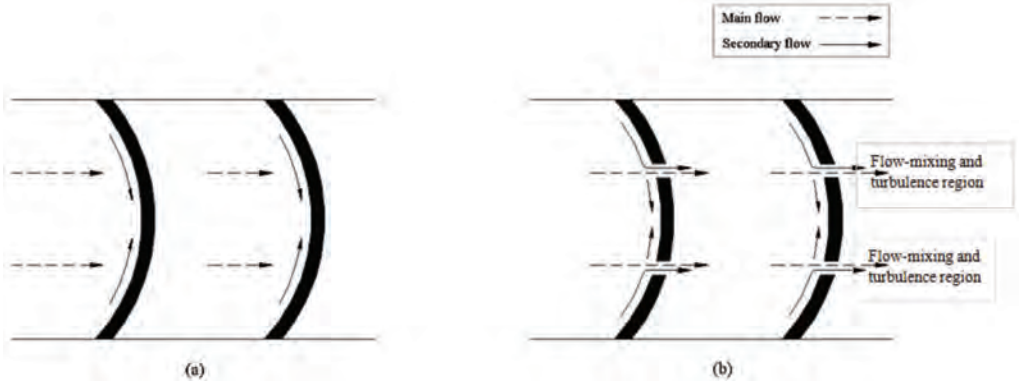


Fig. 7. Flow pattern for continuous arc rib and arc rib having gap

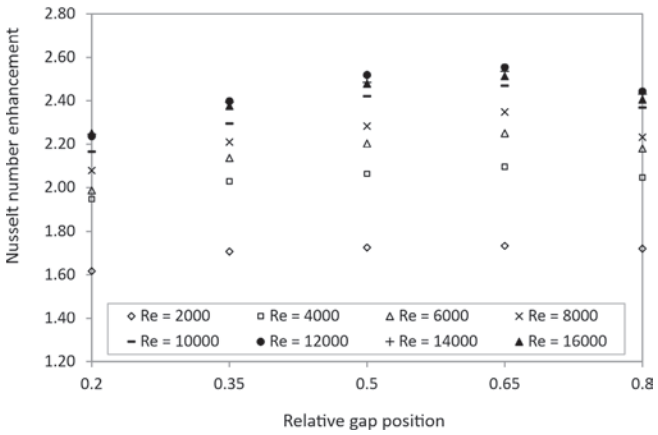


Fig. 8. Nusselt number enhancement as a function of relative gap position

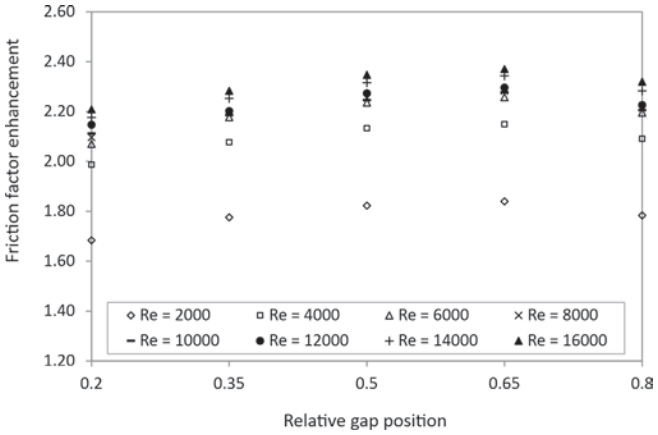


Fig. 9. Friction factor enhancement as a function of relative gap position

www.IndianJournals.com
Not for Commercial Use
Downloaded From IP - 216.73.216.57 on dated 15-Nov-2026

increases, interaction of boundary layer on upstream side of the rib with secondary flow moving along the rib increases which results in the increase in strength of secondary flow. This increased strength of secondary flow through the gap leads to rise in turbulence on downstream of the gap that causes increase in heat transfer. On other hand with the increase in relative gap position, the strength of secondary flow decreases due to decrease in angle at which boundary layer strike the arc rib. This decreased strength of secondary flow through the gap leads to less turbulence on downstream of the gap that causes decrease in heat transfer. In the range of relative gap position from 0.20-0.65, it is anticipated that heat transfer increase, due to increase in strength of secondary flow through the gap caused by increase in interaction of boundary layer with secondary flow, dominates over the decrease in strength of secondary flow through the gap due to decrease in angle at which boundary layer strike the arc rib. Thus, the Nusselt number increased as relative gap position is increased from 0.2 to 0.65. However, for increase in relative gap position beyond 0.65, decrease in strength of secondary flow through the gap caused by decrease in angle at which boundary layer strike the arc rib dominates over increase in strength of secondary flow through the gap due to increase in interaction of boundary layer with secondary flow. Thus, the Nusselt number decreased as relative gap position is increased from 0.65 to 0.80.

In order to clearly present the effect of Reynolds number on Nusselt number enhancement (*Nu/Nus*) and friction factor enhancement (*f/fs*), the results shown in Fig. 8 and Fig. 9 are again drawn in Fig. 10 and Fig. 11. From Fig. 10, It is observed that the Nusselt number enhancement increases with increase in Reynolds number up to 12000 and then decreases with further increase in Reynolds number. The friction factor enhancement also increases with increase in Reynolds number. This is because as the Reynolds

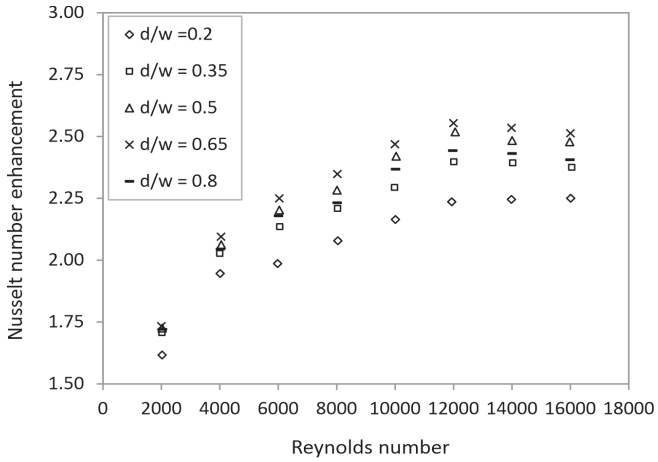


Fig. 10. Nusselt number enhancement as a function of Reynolds number

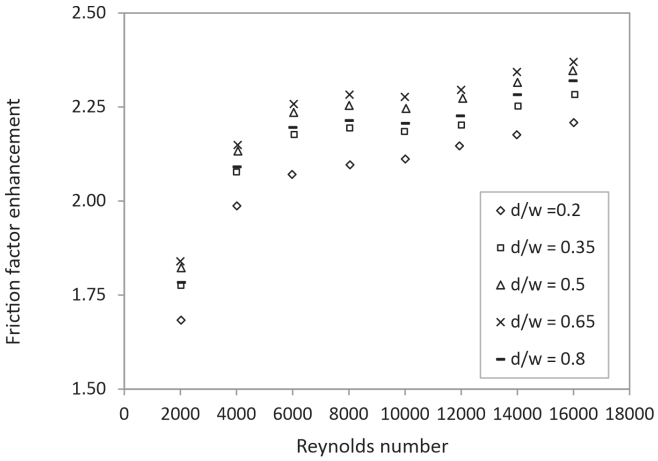


Fig. 11. Friction factor enhancement as a function of Reynolds number

number increases, the roughness elements project more beyond the viscous sublayer due to decrease in thickness of viscous sublayer. At a certain value of the Reynolds number, the thickness of the viscous sublayer becomes very small and energy loss due to vortices attains a constant value, indicating start of fully rough region. Now, the roughened surface behaves like a normal surface with enhanced values of friction factor and Nusselt number. Hence, the slope of curves of Nusselt number enhancement and friction factor enhancement decreases. The maximum enhancement in Nusselt number is 155.4% at the Reynolds number of 12000. The corresponding enhancement in friction factor is 129.6%.

Based on the experimental investigation on broken arc rib roughened solar air heater duct for different relative gap positions, following conclusions can be drawn:

a. The variation in relative gap position has strong influence on Nusselt number and friction factor.

b. For all Reynolds number, the Nusselt number and friction factor enhancement increases with relative gap positions from 0.2 to 0.65 and both decreases with further increase in relative gap positions.

c. The more enhancement in heat transfer as compared to friction factor indicates that it is advantageous to use broken arc rib roughened solar air heater with relative gap position of 0.65 as compared to other values of relative gap positions and smooth surface. The highest value of enhancement of heat transfer and friction factor as compared to smooth duct is 155.4 and 129.6 percent respectively for relative gap position of 0.65 and Reynolds number value of 12000.

www.IndianJournals.com
Not for Commercial Use
Downloaded From IP - 216.73.216.57 on dated 15-Nov-2026

Authors' contribution

Conceptualization of research work and designing of experiments (VSH, RSG); Execution of field/lab experiments and data collection (RSG, RPS); Analysis of data and interpretation (RSG, RPS); Preparation of manuscript (VSH).

Acknowledgements

The authors acknowledge the grant received from University Grants Commission (UGC), India for financially supporting this research work.

LITERATURE CITED

Aharwal K R 2008. *Heat transfer and fluid flow characteristics of discrete rib roughened solar air heaters*. PhD thesis, IIT Roorkee, India.

ASHRAE, Standard 93–97, 1977. *Method of Testing to determine the thermal performance of solar air heater*, American Society for Heating, Refrigeration and Air Conditioning Engineering, NY: 1-34.

Bhatti M S and Shah R K 1987. Turbulent and Transition Flow Convective Heat Transfer in Ducts, In *Handbook of Single-Phase Convective Heat Transfer*, Kakac S, Shah R K and W. Aung, (eds.). John Wiley, New York.

Bhushan B and Singh R 2010. A review on methodology of artificial roughness used in duct of solar air heaters. *Energy* **35**: 202-12.

Chhaparwala G K, Srivastavaa A and Dayal R 2019. Artificial repeated-rib roughness in a solar air heater – A review Author links open overlay panel. *Solar Energy* **194:** 329-59.

Dutta P P and Kumar A 2017. Development and Performance Study of Solar Air Heater for Solar Drying Applications. In *Solar Drying Technology*, Prakash O and Kumar A (eds.). Green Energy and Technology. Springer, Singapore

Gill R S, Hans V S, and Singh R P 2016. Heat transfer and friction characteristics of broken arc ribs roughened solar air heater ducts. *Agric Res J.* **53(1)**: 81-5.

Gupta A D and Varshney L 2017. Performance prediction for solar air heater having rectangular sectioned tapered rib roughness using CFD. *Thermal Science and Engineering Progress* **4**: 122-32.

Han J C, Zhang Y M and Lee C P 1991. Augmented Heat Transfer in Square Channels with Parallel, Crossed, and V-Shaped Angled Ribs. *Trans. of ASME, J. Heat Transfer* **113(3)**: 590-96.

Han J C and Park J S 1988. Developing heat transfer in rectangular channels with rib turbulators. *International Journal of Heat and Mass Transfer* **31**: 183-95.

Han J C, Glicksman L R and Rohsenow W M 1978. An investigation of heat transfer and friction for rib-roughened surfaces. *Int J Heat and Mass Trans* **21**: 1143-56.

Hans V S, Saini R P and Saini J S 2010. Heat transfer and friction factor correlations for a solar air heater duct roughened artificially with multiple V-ribs. *Solar Energy* **84**: 898-911.

Kant R and Saini R P 2018. Nusselt number and friction factor correlations for forced convective type counter flow solar air heater having discrete multi V shaped and staggered rib roughness on both sides of the absorber plate. *Applied Thermal Engineering*, **129**: 735-46.

Karwa R 2003. Experimental studies of augmented heat transfer and friction in asymmetrically heated rectangular ducts with ribs on the heated wall in transverse, inclined, v-continuous and v-discrete pattern. *Int. Comm. Heat Mass Transfer* **30**: 241-50.

Komolafea C A, Oluwaleyeb I O, Awogbemibc O and Osuekea C O 2019. Experimental investigation and thermal analysis of solar air heater having rectangular rib roughness on the absorber plate. *Case Studies in Thermal Engineering* **14:** 100442.

Kumar Anil, Saini R P and Saini J S 2011. Heat transfer and friction characteristics of rectangular solar air heater duct with multi v-shaped ribs with gap roughness on the

absorber plate, *Proc of the 21st National & 10th ISHMT-ASME Heat and Mass Transfer Conference*, IIT Madras, India.

Park J S, Han J C, Huang Y, Ou S and Boyle R J 1992. Heat transfer performance comparisons of five different rectangular channels with parallel angled ribs. *Int J Heat Mass Transfer* **35**: 2891-2903.

Rohsenow W M, Hartnett J P and Cho Y I 1998. *Handbook of heat transfer*. McGraw Hill, New York, 1501p.

Sahu M M and Bhagoria J L 2005. Augmentation of heat transfer coefficient by using 90° broken transverse ribs on absorber plate of solar air heater. *Renewable Energy* **30**: 2057-63.

Sivakandhana C, Arjunanb T V and Matheswaran M M 2020. Thermohydraulic performance enhancement of a new hybrid duct solar air heater with inclined rib roughness *Renewable Energy* **147:** 2345-57.

Sukhatme S P 1996. *Solar Energy: Principles of Thermal Collection and Storage*, Tata McGraw Hill Publishing Company Limited, New Delhi, 431p.

Sukhmeet S, Chander S and Saini J S 2012. Investigations on thermo-hydraulic performance due to flow-attack-angle in V-down rib with gap in a rectangular duct of solar air heater. *Applied Energy* **97**: 907-12.

Varun, Saini R P and Singal S K 2007. A review on roughness geometry used in solar air heaters. *Solar Energy* **81(11)**: 1340-50.

www.IndianJournals.com
Not for Commercial Use
Downloaded From IP - 216.73.216.57 on dated 15-Nov-2026